

The RTM Cascade Framework

Hierarchical Dynamics: Scale-Dependent Stability and Phase Bifurcation

Álvaro Quiceno

Significance & Operationalization (from Concept to Test)

Why this matters. Many multiscale systems *appear* to organize information as it moves across nested layers, but most evidence is confounded by level shifts (gains, delays, kinematics). We separate **coherence** from **level effects** by treating the **log-log slope** $\alpha = \partial \log T / \partial \log L$ as the operational marker of organization, and relegating layer-wide factors to the intercept. This yields a clean, falsifiable question: *does coherence increase (or at least not decrease) along the sequence, and is information flow one-way forward?*

From concept to test. We convert the narrative into two empirical signatures:

S1 — Monotone coherence across layers. Within each layer, regress $\log T$ on $\log L$; the cascade hypothesis requires $\alpha_{n+1} \geq \alpha_n - \varepsilon$ (95% bootstrap CIs; ε pre-registered).

S2 — Forward-only directionality. Estimate **transfer entropy** and **Granger causality** between adjacent layers; require significance forward ($n \rightarrow n + 1$) and not reverse, with surrogate-based p-values and FDR control.

Controls, stress tests, and reproducibility. We include (i) **intercepts-only** controls (flat α with large level shifts), (ii) a **null** with uncoupled layers (no directionality), and (iii) a **hysteresis/ratchet** sweep (supporting evidence of directional memory).

Abstract

While previous papers established the static scaling relationship $T \propto L^\alpha$, this document explores the dynamics of such systems across hierarchical scales. We analyze how energy and information propagate through the "RTM Lattice," proposing a model of **Hierarchical Cascades**. We demonstrate that systems with differing α exponents (e.g., diffusive vs. ballistic) cannot couple efficiently without a transitional interface, leading to **Impedance Mismatch** phenomena. Furthermore, we formalize the upper limits of structural size ("Allometric Instability") and derive the conditions under which a system undergoes **Symmetry Breaking** in its temporal evolution. This framework provides a mechanism for macro-scale structure formation from micro-scale coherence, without invoking exotic physics.

Empirical validation⇒(APPENDIX A). We validate the RTM cascade framework in biological neural systems through an expanded systematic analysis of 21 areas within the visual cortex hierarchy. The analysis evaluates how the temporal processing time (τ) scales with the spatial receptive field size (L). The results reveal a strict topological signature: the system operates in a **Sub-diffusive** scaling regime, yielding an exponent of $\alpha = 0.303 \pm 0.020$ ($R^2 = 0.921, p < 10^{-11}$). This exponent ($\alpha < 0.5$) indicates that the brain integrates information across cortical space mathematically more efficiently than a classical random

diffusion network ($\alpha = 0.5$). By combining parallel processing with hierarchical coding, biology successfully bypasses the physical limits of diffusive transport, validating α as a fundamental metric for quantifying architectural efficiency in complex neural networks.

1. Introduction

1.1 Motivation and scope

RTM (Multiscale Temporal Relativity) posits that the characteristic time of a process scales with an effective size according to $T/T_0 = (L/L_0)^\alpha$, where the exponent α operationalizes **mesoscopic coherence**. The conceptual essays *Simulacrum* and *La Arquitectura del Eco* motivate a picture in which information is **re-encoded** into increasingly ordered structures and propagated **sequentially** across nested layers—an “resonant harmonics architecture” that advances forward rather than backward. Our goal here is to translate that narrative into **testable, falsifiable signatures** that can be probed with real or analog data, without committing to metaphysical claims.

1.2 Problem statement

Given a system decomposable into layers $n = 1, \dots, N$ (spatial shells, functional modules, or controlled analog stages), does **coherence** increase (or at least not decrease) along the sequence, and is the **information flow** predominantly **from n to $n + 1$** ? If so, RTM predicts changes in **slope** $\alpha_n = \partial \log T / \partial \log L$ and **directional causality** between layer observables. If not, slopes should remain invariant and causal metrics should be symmetric.

1.3 Testable signatures (what this paper measures)

We focus on two empirical handles:

- **(S1) Slope-based coherence:** in each layer, regress $\log T$ on $\log L$ to estimate α_n with bootstrap CIs. The cascade hypothesis requires $\alpha_{n+1} \geq \alpha_n - \varepsilon$ for small tolerance ε .
- **(S2) Directional causality:** quantify **transfer entropy** (TE) and/or **Granger causality** between time series derived from adjacent layers; expect significance for $n \rightarrow n + 1$ and not conversely.

Optional extensions we will explore include **ratchet/hysteresis** under control sweeps of the inter-layer coupling and a **coherence-disorder trade-off** (increase in α alongside a reduction of activity-entropy).

1.4. Systematic Empirical Validation: The Sub-diffusive Regime of the Visual Cortex⇒(APPENDIX A)

Within the theoretical framework of RTM, hierarchical cascade architectures (such as the human brain) do not merely process information; they must navigate fundamental topological constraints of space and time. To subject this premise to an empirical test, we analyzed the scaling relationship between the spatial extent of the receptive field (L) and the temporal processing latency (τ) across 21 distinct areas of the visual hierarchy.

The central question is: What class of physical transport does biology utilize to integrate this information? The data overwhelmingly reveal that the visual cortex does not operate under the inefficiency of random diffusion ($\alpha = 0.5$), but has evolved toward a highly optimized and **Sub-diffusive** regime ($\alpha \approx 0.30$). This finding demonstrates that the brain's macroarchitecture, driven by massive parallel processing at each hierarchical level, manages to "bend" the classical rules of statistical physics to achieve hyper-efficient information integration, effectively bridging the boundary between diffusive and ballistic kinetics.

2. Essential mathematical formulation

2.1 RTM scaling on layered systems

We consider a system decomposed into N nested **layers** $n \in \{1, \dots, N\}$. On each layer, a mesoscopic process time T_n associated with an effective size L follows the RTM law

$$\frac{T_n}{T_0} = \left(\frac{L}{L_n} \right)^{\alpha_n} \Xi_n \quad (2.1)$$

where:

- α_n is the **coherence exponent** for layer n (the quantity we wish to estimate);
- T_0, L_n are reference scales (fixed across layers);
- Ξ_n is a **layer-level factor** that shifts levels but **does not depend on L** (e.g., redshift/kinematics in astrophysical settings, instrumental latency, layer-wide gain).

Taking logs,

$$\underbrace{\log T_n}_{y_n} = \underbrace{\alpha_n}_{\text{slope}} \cdot \underbrace{\log L}_{x} + \underbrace{\log(T_0/L_0^{\alpha_n}) + \log \Xi_n}_{\beta_n} + \quad (2.2)$$

so at **fixed layer n** the **log-log slope** equals α_n and the **intercept** β_n absorbs Ξ_n . This is the basis for Signature (S1) (slope-based coherence). Conceptually, α captures **organization/coherence**, consistent with the "re-encoding" narrative that motivates this work.

2.2 Estimation target and regression model

Given observations $\{(L_{ni}, T_{ni})\}_{i=1}^{m_n}$ on layer n spanning a range of sizes L , we estimate

$$\alpha_n = \frac{\partial \log T_n}{\partial \log L} \Big|_n$$

via **ordinary least squares (OLS)** in the model (2.2). We report:

- point estimate $\hat{\alpha}_n$,

- **95% bootstrap CIs** (resampling events within layer n),
- goodness-of-fit diagnostics (residuals vs. $\log L$).

Design note. Identifiability of α_n requires **spread** in L within the layer ($\geq 6\text{--}8$ distinct sizes is a good rule of thumb).

2.3 Directional information flow between layers

Let $X_n(t)$ denote a layer-specific observable series (e.g., event rate, pulse energy, width). Signature **(S2)** tests whether **causal influence** is **asymmetric** from $n \rightarrow n + 1$.

(a) Transfer entropy (TE)

For lags k and l ,

$$\text{TE}_{n \rightarrow n+1} = \sum p(x_{n+1}(t+1), x_{n+1}^{(k)}(t), x_n^{(l)}(t)) \log \frac{p(x_{n+1}(t+1) \mid x_{n+1}^{(k)}(t), x_n^{(l)}(t))}{p(x_{n+1}(t+1) \mid x_{n+1}^{(k)}(t))} \quad (2.3)$$

We test $\text{TE}_{n \rightarrow n+1} > \text{TE}_{n+1 \rightarrow n}$ using permutation/bootstrap surrogates to obtain p-values.

(b) Granger causality (G-test)

In a bivariate VAR with order p ,

$$X_{n+1}(t) = \sum_{j=1}^p a_j X_{n+1}(t-j) + \sum_{j=1}^p b_j X_n(t-j) + \eta(t) \quad (2.4)$$

We test $H_0: b_1 = \dots = b_p = 0$ (no Granger causality $n \rightarrow n + 1$). Directionality requires significance for $n \rightarrow n + 1$ and **not** for $n + 1 \rightarrow n$.

Interpretation. A forward “resonant harmonics architecture” implies **non-decreasing coherence** ($\alpha_{n+1} \geq \alpha_n - \varepsilon$) together with **asymmetric information flow** $n \rightarrow n + 1$.

2.4 Hypotheses and falsification criteria

Slope (S1).

- $H_0: \alpha_{n+1} < \alpha_n - \varepsilon$ for some adjacent pair (decrease beyond tolerance).
- $H_1: \alpha_{n+1} < \alpha_n - \varepsilon$ for all n .

Decision: Reject support if any adjacent CI for $\hat{\alpha}_{n+1} - \hat{\alpha}_n$ lies **entirely below** $-\varepsilon$

Directionality (S2).

- H_0 : symmetry or reverse influence, $\text{TE}_{n \rightarrow n+1} \leq \text{TE}_{n+1 \rightarrow n}$ (and similarly for Granger).

- H_1 : forward asymmetry, $TE_{n \rightarrow n+1} > TE_{n+1 \rightarrow n}$ (**and** G-test significant only forward).
Decision: Require both TE and Granger to agree on forward asymmetry (with multiple-comparison control across n).

2.5 Controls and confounders (intercepts vs slopes)

Layer-level factors \mathcal{E}_n (e.g., gravitational/kinematic mapping, global gains) act **only on the intercept** β_n in (2.2). Therefore:

- **Intercept changes** across layers do **not** imply coherence change.
- **Slope changes** indicate RTM-relevant organization.
 This disentangles “clock mapping”/instrumental effects from coherence, exactly as in the prior RTM study of compact environments.

2.6 Noise, robustness, and proxies for L

- **Noise model.** We assume multiplicative fluctuations: ε log-normal with scale $\sigma_{log} \in [0.05, 0.2]$. Bootstrap CIs mitigate non-Gaussianity.
- **Outliers.** If heavy tails are suspected, complement OLS with **Theil-Sen** or Huber-regression sensitivity checks.
- **Proxies for L.** When L is not directly measured, define **geometric, kinematic** ($L \approx vT_{rise}$), or **statistical** proxies (correlation length). Report slopes for **multiple proxies** and check stability.

2.7 Parametric templates for simulations/analytics

For synthetic and analog studies we use a monotone profile for coherence across layers:

$$\alpha_n = \alpha_{base} + \Delta\alpha \frac{1}{1+\exp\left(\frac{(n-n_c)}{w}\right)} \quad (\text{logistic}), \quad \text{or} \quad \alpha_n = \alpha_{base} + \Delta\alpha \left(\frac{n_c}{\max(n, n_c)}\right)^p \quad (\text{soft ramp}) \quad (2.5)$$

Directional coupling is introduced only from n to $n + 1$ (for S2), with a tunable strength g used later to probe **ratchet/hysteresis**.

2.8 Power and design guidance

- **Within-layer span in L** dominates power for α_n : target $\geq 6-8$ distinct sizes per layer and ≥ 1 decade span when possible.
- **Series length for TE/Granger:** at least $10^2 - 10^3$ effective samples per layer pair, with cross-validation on lag orders.
- **Pre-registration:** (i) tolerance ε ; (ii) lag orders for TE/Granger; (iii) multiple-comparison control; (iv) criteria for null acceptance.

Provenance and delimitation. The layered “resonant harmonics” picture comes from *La Arquitectura del Eco*; the **information re-encoding** intuition from *Simulacrum*. Here we restrict both to **operational signatures** (slopes, causal asymmetry) that can be confirmed or refuted with data from real or analog systems.

3. Testable predictions and decision rules

This section turns the layered RTM formulation (§2) into **concrete, falsifiable predictions** with explicit tests, thresholds, and stopping rules. The predictions are grouped as **core** (must pass) and **supporting** (strengthen the claim but are not required). Conceptual provenance—*Simulacrum* (re-encoding) and *La Arquitectura del Eco* (sequential “resonant harmonics”)—is kept as **motivation only**; the tests below stand on operational grounds.

3.1 Core signature S1 — Monotone coherence across layers (slope test)

Prediction. Along the layer index $n = 1, \dots, N$, the coherence exponent is **non-decreasing** within tolerance ε :

$$\Delta\alpha_n \equiv \alpha_{n+1} - \alpha_n \geq -\varepsilon \quad \text{for all } n \tag{3.1}$$

Estimator. For each layer n , fit $\log T_{log} = \alpha_n \log L + \beta_n + \varepsilon$ (Eq. 2.2), obtain $\hat{\alpha}_n$ and a 95% **bootstrap CI** (resampling events within layer n , ≥ 1000 replicates).

Layerwise test. For each adjacent pair,

$$\widehat{\Delta}\alpha_n = \hat{\alpha}_{n+1} - \hat{\alpha}_n, \quad \text{with bootstrap CI } [\text{lo}_n, \text{hi}_n] \tag{3.2}$$

Pass if $\text{lo}_n \geq -\varepsilon$ for all n . **Fail** (falsification) if any $\text{hi}_n < -\varepsilon$

Global test (optional robustness). Fit an **isotonic regression** (non-decreasing α_n) and compare against unconstrained fits via a **likelihood-ratio bootstrap**; reject monotonicity if the constrained model is significantly worse (e.g., $p < 0.05$).

Design notes. Power is dominated by the **span in L** per layer (§2.8). Target $\geq 6 - 8$ distinct L values and \geq one decade span.

3.2 Core signature S2 — Directional causality (forward resonant harmonics)

Let $X_n(t)$ be a layer-specific time series (rate, pulse energy, widths, or a feature extracted consistently across layers).

Prediction. Information flow is **asymmetric forward**:

$$\text{TE}_{n \rightarrow n+1} > \text{TE}_{n+1 \rightarrow n} \quad \text{and} \quad \text{Granger}(n \rightarrow n+1) \text{ significant, Granger}(n+1 \rightarrow n) \text{ not.} \quad (3.3)$$

Transfer entropy (TE). Estimate $\text{TE}_{n \rightarrow n+1}$ and $\text{TE}_{n+1 \rightarrow n}$ with matched embedding; obtain p-values via **permutation/phase-shuffle surrogates** (≥ 1000). Apply **BH-FDR** across pairs.

Granger. Fit a bivariate VAR with order selected by AIC/BIC. Test H_0 (no Granger) via F-test. Require significance **only** for the forward direction.

Decision rule. Claim **forward resonant harmonics** only if **both** TE and Granger agree on forward asymmetry after multiple-comparison control. Otherwise: **no support** for directionality.

Design notes. Use $\geq 10^2 - 10^3$ effective samples per pair; cross-validate lags; check stationarity (difference/detrend if needed).

3.3 Supporting signature S3 — Ratchet/hysteresis under coupling sweeps

Introduce a controllable inter-layer coupling g (analog platform). Sweep g **up** and then **down**, measuring $\hat{\alpha}_{n+1}(g)$.

Prediction. Hysteresis loop: the forward and backward branches differ (one-way activation memory).

Quantification. Define loop area

$$\mathcal{A}_{n+1} = \oint \hat{\alpha}_{n+1}(g) dg \quad (3.4)$$

(discrete trapezoids). **Pass** if \mathcal{A}_{n+1} differs from zero beyond bootstrap CI; **fail** if consistent with zero.

3.4 Supporting signature S4 — Coherence-disorder trade-off

Define a **dynamic-disorder** metric on each layer (choose one, pre-register): (i) Shannon entropy of inter-event intervals; (ii) spectral entropy; (iii) permutation entropy.

Prediction. Across layers,

$$\text{corr}(\Delta \hat{\alpha}_n, -\Delta \hat{S}_{dyn,n}) > 0, \quad (3.5)$$

i.e., increases in coherence (slope) accompany reductions in dynamic disorder under the same coarse-graining (operational “re-encoding” narrative). Test with **Spearman** (robust to nonlinearity) and report CIs via bootstrap.

3.5 Joint decision logic (pre-registered)

- **Support:** S1 and S2 pass.
- **Strengthened support:** S1 & S2 pass and at least one of S3/S4 passes.
- **Null / falsification:** S1 fails (significant slope drop $< -\varepsilon$) or S2 fails (no forward asymmetry). S3/S4 informative but not required.

Set ε by instrument/design (e.g., $\varepsilon = 0.05 - 0.1$ in α units), pre-register lag ranges and surrogate counts for TE, and apply BH-FDR across all pairwise tests.

3.6 Robustness and confounder controls

- **Intercept vs slope.** Differences in layer-level factors Σ_n (redshift/kinematics; global gains) affect **intercepts** only (§2.5). Do **not** interpret intercept shifts as coherence changes.
- **L proxies.** Report slopes for **multiple L proxies** (geometric/kinematic/statistical); claim S1 only if conclusions are stable.
- **Window tests.** Refit slopes after (i) dropping the largest L ; (ii) using only the top-k sizes; (iii) Huber/Theil-Sen fits to guard against outliers.
- **Causality sensitivity.** Repeat TE/Granger with (i) different embeddings/lags; (ii) surrogate types (time-shuffle vs phase-randomized); (iii) downsampled data to test temporal resolution effects.
- **Negative controls.** Include a **null segment** with intentionally decoupled layers; require S2 to be null there.

3.7 Minimal reporting checklist (for methods/results)

1. L proxies (definitions, uncertainties) and within-layer span.
2. $\hat{\alpha}_n$ with 95% bootstrap CIs; pairwise $\hat{\Delta}\alpha_n$ with CIs.
3. TE/Granger settings (lags, embeddings), surrogate counts, adjusted p-values.
4. S3/S4 metrics (if used), including bootstrap CIs and effect sizes.
5. Robustness outcomes (proxy changes, window tests, alternative regressions).
6. Pre-registered ε , multiple-comparison control, and **falsification rule**.

What would not count as support. Flat slopes across layers with only intercept differences; TE/Granger symmetry; hysteresis area \mathcal{A} consistent with zero; no coherence-disorder correlation. Any of these negate the sequential-coherence (resonant harmonics) interpretation **in that system**, irrespective of motivational narratives.

4. Simulations and synthetic controls (E1–E4)

This section validates the two core signatures—**(S1)** monotone coherence across layers (slope test) and **(S2)** forward directionality (TE/Granger)—using lightweight synthetic models. Each experiment specifies: **model**, **measurement**, **decision rule**, and **typical outcome patterns**. We also include stress tests and a minimal reproducibility pack.

4.1 E1 — Four-layer cascade with non-decreasing coherence (S1)

Model. Layers $n \in \{1,2,3,4\}$ with

$$T_n = \Xi_n T_0 \left(\frac{L}{L_0} \right)^{\alpha_n} \varepsilon, \quad \alpha_n = \alpha_{\text{base}} + \Delta\alpha \cdot \frac{1}{1 + \exp(n - n_c/w)}$$

Here Ξ_n is a layer-level factor independent of L (level/“clock mapping” only); $\log \varepsilon \sim N(0, \sigma_{\log}^2)$. Choose L on a geometric grid (≥ 8 – 10 sizes per layer; ≥ 1 decade span).

Measurement. Within each layer n , regress $\log T$ on $\log L$ (OLS), report $\hat{\alpha}_n$ and 95% bootstrap CIs (resample events within n , ≥ 1000 reps). Compute adjacent differences $\hat{\Delta}\alpha_n = \hat{\alpha}_{n+1} - \hat{\alpha}_n$ with CIs.

Decision rule (S1). Pass if all $lo(\hat{\Delta}\alpha_n) \geq -\varepsilon$. Optional global check: isotonic (non-decreasing) fit for α_n is not significantly worse than the unconstrained one (bootstrap LR).

Typical pattern. $\hat{\alpha}_n$ rises (or plateaus) with n ; CIs do not show significant drops; intercepts differ across layers but do not affect slopes.

4.2 E2 — Directional causality in a layered chain (S2)

Model. Layer observables $X_n(t)$ obey a **forward-coupled** bivariate (pairwise) process between neighbors:

$$\begin{aligned} X_{n+1}(t) &= \sum_{j=1}^p a_j X_{n+1}(t-j) + \sum_{j=1}^p b_j X_n(t-j) + \eta_{n+1}(t), \\ X_n(t) &= \sum_{j=1}^p c_j X_n(t-j) + v_n(t), \end{aligned}$$

with $b_j \neq 0$ (forward), no back-coupling in this experiment. Generate $\sim 10^3$ samples/layer pair; match lag orders by AIC/BIC.

Measurement.

- **TE:** estimate $TE_{n \rightarrow n+1}$ and $TE_{n+1 \rightarrow n}$ with matched embeddings; obtain p -values via surrogate tests (permutation/phase-shuffle, ≥ 1000).

- **Granger:** F-tests on b_j vs. 0; check reverse direction separately.

Decision rule (S2). Claim forward directionality if **both** TE and Granger are significant for $n \rightarrow n + 1$ and **not** for $n + 1 \rightarrow n$ (FDR-adjusted).

Typical pattern. $TE_{n \rightarrow n+1} \gg TE_{n+1 \rightarrow n}$; Granger significant only forward. When the forward coupling is reduced, both metrics decrease smoothly toward the null.

4.3 E3 — Ratchet/hysteresis under coupling sweeps (supporting S3)

Model. Introduce a controllable coupling $g \in [g_{min}, g_{max}]$ that modulates either $\alpha_{n+1}(g)$ (through effective organization) or the forward coefficients $b_j(g)$. Sweep g **up** and then **down**, allowing a slow internal state to produce memory.

Measurement. Track $\hat{\alpha}_{n+1}(g)$ (slope per layer at each g) and compute the **loop area** $\mathcal{A}_{n+1} = \oint \hat{\alpha}_{n+1}(g) dg$ using trapezoidal integration.

Decision rule (S3). Pass if \mathcal{A}_{n+1} 's bootstrap CI excludes 0 (directional memory); otherwise **no ratchet**.

Typical pattern. The forward branch shows earlier/larger $\hat{\alpha}$ activation than the backward branch; loop area > 0 within CI.

4.4 E4 — Null controls (flat slopes and symmetric causality)

Model. Hold $\alpha_n \equiv \alpha_*$ constant for all n and set couplings symmetric or zero. Keep layer factors Ξ_n heterogeneous to ensure intercept differences remain present.

Measurement and decision.

- **S1:** Adjacent $\hat{\Delta}\alpha_n$ CIs include 0 (no monotone trend).
- **S2:** TE and Granger are symmetric or non-significant after FDR.

Typical pattern. Flat $\hat{\alpha}_n$ across layers with non-zero intercept shifts; TE/Granger do not show a favored direction—this safeguards against false positives.

4.5 Stress tests (robustness and failure modes)

- **Proxy noise for L .** Replace true L by proxies with multiplicative error; **slope** remains stable when errors are i.i.d. within a layer; severe, layer-dependent bias can mimic $\Delta\alpha$ (flag via alternative proxies and window tests).
- **Span in L .** Reducing the L range inflates CIs; power drops steeply below ~ 6 distinct sizes/layer or < 0.5 decades span.
- **Heteroskedastic/heavy-tailed noise.** Use bootstrap CIs; run Huber/Theil-Sen sensitivity—claims must persist.

- **Mis-binning across layers.** Mixing distinct E_n within a layer can bleed level effects into slope estimates; mitigate with narrow bins and consistent proxy definitions.
- **Causality settings.** TE/Granger are sensitive to embedding/lags; pre-register ranges and verify directionality under multiple reasonable choices; use surrogates rigorously.

4.6 Minimal reproducibility pack

We release (i) scripts to generate data for E1–E4 with a fixed RNG seed, (ii) OLS+bootstrap slope estimators, (iii) TE/Granger routines with surrogate testing, and (iv) plotting scripts. Outputs include per-layer CSVs ($\hat{\alpha}_n$, CIs, TE/Granger metrics) and PNG figures for each experiment. A short **README** documents inputs, parameters, and the decision logic (S1–S2, plus S3/S4 when used).

Summary of synthetic outcomes

Across E1–E4 the pipeline behaves as intended: when a forward cascade is present, **slopes are non-decreasing** and **causal flow is asymmetric**; when it is absent, **slopes are flat** and **directionality vanishes**, despite intercept shifts. These controls show that the layered RTM program yields **sensitive** and **specific** empirical signatures, setting the stage for laboratory analogs and observational analyses.

5. Analog experiments (design & protocols)

This section turns the RTM cascade into **laboratory protocols** that can produce the two core signatures: **(S1)** non-decreasing slope α_n across layers and **(S2)** forward-only information flow (TE/Granger). Each platform defines: **layers**, an **effective size proxy** L , a **mesoscopic time** T , a **directional coupling** $n \rightarrow n + 1$ with tunable strength g , and a measurement pipeline that isolates **slope (coherence)** from **intercept (level/clock mapping)**.

5.1 Platform A — Directional chain of coupled resonators (optical / RF / mechanical)

Goal. Realize N nested layers as a **series of resonators** with **one-way coupling**. Examples:

- **Optical:** fiber-ring or micro-ring cavities linked by **optical isolators** or circulators.

- **RF/microwave:** superconducting or room-temp cavities with **circulators** (non-reciprocal).
- **Mechanical:** weakly coupled cantilevers/mass-spring resonators with active **unidirectional feedback**.

Layer definition & observables.

- **Layer n :** the $n - th$ resonator.
- **Size proxy L :** injected **pulse width** (temporal), or **spectral bandwidth** (frequency) treated as an effective “scale.” Use $\geq 6 - 8$ distinct L per layer.
- **Mesoscopic time T :** cavity **ring-down time**, **damping time**, or **first-passage/escape time** of the pulse envelope.

Control & directionality.

- **Unidirectionality:** isolator/circulator between n and $n + 1$; block $n + 1 \rightarrow n$.
- **Coupling strength g :** set by coupler transmissivity / coupling capacitance / feedback gain. Sweep g (up & down) for **hysteresis** (S3).

Acquisition.

- Inject pulse families at **each layer** (or only at the first if cascading the same pulse).
- For each n , collect m_n events per L (target $m_n \geq 30$) and sample time-series $X_n(t)$ (e.g., envelope or energy) at $\geq 10 \times$ the fastest dynamics.

Analysis.

- **S1:** OLS of $\log T$ vs $\log L$ per layer $\rightarrow \hat{\alpha}_n + 95\% \text{ bootstrap CIs}$. Check $\hat{\Delta}\alpha_n = \hat{\alpha}_{n+1} - \hat{\alpha}_n$ CIs $\not\prec -\varepsilon$.
- **S2:** Compute **TE** ($n \rightarrow n + 1$) vs ($n + 1 \rightarrow n$) with surrogate p-values; run **Granger** (bivariate VAR) with order chosen by AIC/BIC. Require forward-only significance (BH-FDR).
- **S3 (optional):** plot $\hat{\alpha}_{n+1}$ for up/down sweeps; bootstrap the **loop area \mathcal{A}** and test $\mathcal{A} \neq 0$.

Confounder control.

- **Intercept vs slope:** losses and path gains change **intercepts; only slopes** diagnose coherence.
- **Phase/group delay:** treat as a separate level factor Ξ_n ; keep it fixed within each slope fit.
- **Stationarity:** detrend the time-series before TE/Granger; verify with unit-root tests.

Pass/Fail. **Pass** if $\hat{\alpha}_n$ is non-decreasing within ε **and** forward-only causality is significant.
Fail if any adjacent slope drop $< -\varepsilon$ or directionality is symmetric.

5.2 Platform B — Cascaded fluid/phononic waveguides with increasing confinement

Goal. Build a **nested channel** (e.g., water flume with baffles, acoustic/phononic waveguides) where confinement **increases** downstream.

Layer & observables.

- **Layer n :** segment between baffles (or the n -th waveguide cell).
- **Size proxy L :** injected **blob diameter** (fluid), spatial **packet width** (acoustic), or **dominant wavelet scale** from imaging.
- **Mesoscopic time T : transit / escape / ring-down** time measured by high-speed video or pressure/acoustic sensors.

Control.

- **Confinement index g :** nozzle width, baffle spacing, or cavity finesse → **monotone** across layers.
- **Directionality:** flow-imposed or diode-like acoustic elements to suppress back-propagation.

Acquisition & analysis.

- Replicate the **S1** slope protocol per layer with $\geq 6 - 8$ sizes L .
- For **S2**, compute TE/Granger between upstream–downstream sensors.
- Record Reynolds/Froude numbers to document regime; keep them **constant within a run** (intercept factor).

Confounders.

- **Turbulence on/off:** report regime; if turbulence varies layer-wise, treat it as ε_n (intercept) and check slope stability.
- **Imaging bias:** calibrate blob/wavelet L against a target; run **proxy sensitivity** (geometric vs. statistical L).

Pass/Fail. As in 5.1.

5.3 Platform C — Electronic ladder (RLC/active) with one-way coupling

Goal. An **accessible benchtop** realization: a chain of RLC cells (layers) with **active non-reciprocal links** (op-amp buffers / gyrators / diode networks) to emulate one-way coupling.

Layer & observables.

- **Layer nnn:** n -th cell output node.
- **L proxy:** input pulse **width** or **filter bandwidth** (set by RC).
- **T :** decay time (envelope $1/e$), rise/settle time, or first-passage threshold time.

Control.

- **Coupling g :** controllable resistor/gain in the forward path only. Include an up/down sweep for **hysteresis**.

Analysis & confounders.

- Apply the same **S1/S2** pipeline; characterize **noise floor** and **ADC sampling** as level factors.
- Use **Theil-Sen** robustness if outliers appear; confirm slope stability when dropping the largest L .

5.4 Measurement checklist (per platform)

1. **Within-layer L -span:** $\geq 6 - 8$ distinct sizes; aim for ≥ 1 decade.
2. **Replicates:** $m_n \geq 30$ events per L per layer for reliable bootstrap CIs.
3. **Time-series length (S2):** $10^2 - 10^3$ effective samples per adjacent pair; pre-register lag ranges.
4. **Directionality hardware:** isolators/circulators/diodes documented; back-path attenuation measured (dB).
5. **Controls:** include a **null segment** (reciprocal or uncoupled) to verify that S2 returns symmetry.

5.5 Data & analysis pipeline (pre-registered)

- **Pre-processing:** detrend, band-limit if needed; time-stamp events; compute T from consistent thresholds.
- **Slope fits:** OLS on $\log T - \log L$ CIs; window tests (drop largest L , top- k sizes).

- **Causality:** TE with permutation/phase-shuffle surrogates; Granger with AIC/BIC order selection; **BH-FDR** correction.
- **Decision:** S1 pass if all $\text{lo}(\hat{\Delta}\alpha_n n) \geq -\varepsilon$; S2 pass if forward-only significant.
- **Artifacts log:** document any layer-specific Ξ_n shifts (gains, delays, regime changes).

5.6 Expected patterns and failure modes

Supportive patterns. $\hat{\alpha}_n$ monotone (rise/plateau) across layers; TE/Granger significant forward-only; hysteresis area $A > 0$ when sweeping g .

Non-supportive patterns. Flat or **decreasing** $\hat{\alpha}_n$ beyond $-\varepsilon$; TE/Granger symmetric; $A \approx 0$ after sweeps; slope conclusions fragile to L proxy choice.

5.7 Practical considerations, safety, and ethics

- **Safety:** laser/optical isolation (OD eyewear), high-voltage precautions in RF/electronics, splash/impeller safety for fluids.
- **Open materials:** release CAD/schematics, BOM, firmware, acquisition scripts, and analysis notebooks (with seeds) to enable replication.
- **Registration:** pre-register ε , lag ranges, and null segments; archive raw data and code.

Bottom line. The three platforms above provide **independent routes** to test the RTM **sequential-coherence** hypothesis under controlled conditions. A positive result requires **both** slope monotonicity (S1) and forward-only causality (S2); a null or mixed result argues against the Resonant Harmonics -cascade interpretation **in that platform**—precisely the falsifiability standard we want.

6. Discussion

6.1 What a positive result would mean

A consistent **increase (or non-decrease)** of $\hat{\alpha}_n$ across layers **and a forward-only** TE/Granger signal indicates that:

- Coherence (as captured by the RTM slope) **accumulates** along the sequence; and
- The **causal influence** propagates **from** layer n **to** $n + 1$, not symmetrically.

In operational terms, the system is performing a **sequential re-encoding** of dynamics into increasingly organized mesoscopic behavior. This is exactly the empirical reading of the conceptual “resonant harmonics architecture”: the metaphor of “transmutation of information into a more ordered code” becomes a concrete **slope-and-directionality** signature.

Consequences. A positive result warrants:

- Mapping α_n vs. n as a new **structural diagnostic** (comparable across platforms).
- Studying how α depends on control variables (confinement, coupling, stratification), to infer **response curves** and potential **critical points**.
- Beginning a microphysical program to **derive** α from effective interactions (e.g., hierarchical coupling, phase-locking, transport suppression), rather than treating it as a purely phenomenological exponent.

6.2 What a null or mixed result would mean

If (i) layerwise slopes remain **flat** (CIs on $\Delta\hat{\alpha}$ include zero or are negative beyond tolerance) and/or (ii) TE/Granger is **symmetric**, the Resonant Harmonics -cascade hypothesis is **not supported** in that system. This is not a failure of the method: it is the desired falsifiability. Practically:

- Focus shifts to **why** coherence does not accumulate: insufficient coupling, counter-flows, proxy mismatch for L , or intrinsic physics that simply lacks a one-way cascade.
- Negative results in analogs help **sharpen** designs for subsequent runs (e.g., stronger non-reciprocal links, wider span in L , longer time series).

6.3 Intercepts vs. slopes and the ledger separation

Across all analyses, **intercepts** absorb level factors (clock mapping, global gains, regime baselines) and are **not** evidence of organizational change. **Slopes** are the coherence ledger. This separation is the main reason the approach remains compatible with standard dynamics (e.g., GR in astrophysical settings): you can have large intercept shifts without touching α .

6.4 How to read α microphysically

While α is measured statistically, it plausibly encodes:

- **Transport mode:** ballistic ($\alpha \approx 1$) → diffusive ($\alpha \approx 2$) → **super-compressed** mesoscopic times at larger α .
- **Phase organization:** stronger phase-locking or feedback alignment can **raise** α by reducing effective degrees of freedom at a given scale.
- **Multiscale confinement:** nested traps/waveguides/cavities promote **hierarchical** coupling that steepens the time-size law.

Future theory should connect α to **coarse-grained equations** (e.g., generalized diffusion with memory kernels; coupled-oscillator networks with directed links) to predict how α changes under controlled modifications of the medium.

6.5 Cross-domain reach

The same pipeline—layered slope estimation + TE/Granger—applies to:

- **Laboratory analogs:** optical/RF/mechanical resonator chains; fluid/phononic guides with increasing confinement (as designed in §5).
- **Observational systems:** any environment with **stratified layers or modules** where families of processes can be measured over a range of effective sizes L (e.g., spatial shells, altitude bands, nested regions).

The crucial requirement is a **within-layer span in L** sufficient to fit a slope with useful uncertainty, and time-series long enough to estimate directionality.

6.6 Pitfalls and how to avoid them

- **Narrow L span / too few sizes:** inflates CIs and hides trends. *Mitigation:* design for $\geq 6\text{--}8$ distinct LLL per layer and $\geq 0.5\text{--}1$ decade of span.
- **Proxy drift for L :** different proxies across layers can mimic $\Delta\alpha$. *Mitigation:* report **multiple proxies** and require stability of conclusions.
- **Layer mis-binning:** mixing distinct regimes within a layer can leak level effects into slopes. *Mitigation:* narrower bins; document regime indicators as part of \mathcal{E}_n .
- **Causality overfitting:** TE/Granger are sensitive to embeddings/lags. *Mitigation:* pre-register lag ranges; use surrogate tests; apply FDR across pairs.

- **Small-N bias in TE:** short time series inflate false asymmetries. *Mitigation:* downsampling tests, block-bootstrap CIs, and negative-control segments with known symmetry.

6.7 Relation to the motivating narratives

Conceptual language about **re-encoding** and “simulacrum” remains **motivation**, not an empirical claim. This paper’s claims stand or fall on **two observables**: (S1) **non-decreasing slopes** across layers; (S2) **forward-only directionality**. Positive evidence would **motivate** deeper exploration of re-encoding mechanisms; null evidence would **bound** those narratives without prejudice.

6.8 What this enables next

- A **benchmark suite**: publish slopes $\hat{\alpha}_n$, CIs, and TE/Granger tables for each platform/source—enabling direct comparison across labs and datasets.
- **Response maps**: measure $\alpha_n(g)$ as a function of coupling/confinement to identify **operating regions** where coherence gains are largest.
- **Toward derivations**: use empirical α maps to constrain candidate **effective models** (memory kernels, directed coupling graphs, multiscale transport).
- **Engineering angle**: if monotone α and forward TE are robust, one can aim to **design** cascades that purposely **raise** α layer by layer for control or information-processing tasks—clearly marked as engineering follow-up, not part of the present claims.

Bottom line. The RTM cascade is now a **testable** story: either **slopes rise (or hold) forward** and **causality points forward**, or they don’t. Both outcomes are scientifically valuable—one opens a microphysical and engineering program; the other cleanly rules out a seductive but unneeded narrative for that system.

7. Structural Divergence and Phase Space Bifurcation

7.1 From Local Coherence to Global Topology

In the preceding sections, we established the cascade as the organizing principle through which coherence propagates across scales. However, this propagation is subject to stability

constraints. Each node in the cascade represents a locus of **dynamic stability** whose persistence depends on phase alignment with its adjacent domains.

When these alignments drift beyond a critical threshold, the system's trajectory in phase space (Γ) loses uniqueness. The manifold of possible evolutions refracts into multiple stable attractors.

This section formalizes this phenomenon not as a metaphysical divergence, but as **Phase Space Bifurcation**: a structured separation of trajectories driven by the internal dynamics of α -coupling.

7.2 Mechanisms of Phase Separation

Within the RTM formalism, coherence is a scale-dependent function. When the coupling coefficient between adjacent layers falls below a critical value (C_{crit}), the system undergoes **Spontaneous Symmetry Breaking**.

Let the state vector of a layer be $\varphi_n(t)$. The condition for continuity is:

$$C_{n,n+1}(t) = \cos[\varphi_{n+1}(t) - \varphi_n(t)] \geq C_{crit}$$

When $C_{n,n+1} < C_{crit}$, the causal correspondence between layers degrades. The "divergence" is essentially a **decoherence event**: the layers decouple and evolve along distinct thermodynamic trajectories.

What is often modeled in cosmology as "distinct bubbles" can be rigorously described here as **orthogonal phase harmonics** within a single high-dimensional state space.

7.3 Allometric Structural Instability (The Impedance Limit)

A critical constraint on this coupling is the **Allometric Instability**.

Just as biological structures obey square-cube laws, temporal structures obey **Information Latency Limits**.

If the scaling difference between two domains ($\Delta \alpha$) exceeds a structural threshold ($\Delta \alpha > 0.5$), the metric scaling ratio becomes incompatible:

$$\rho_{eff} \propto k^{-4\Delta \alpha}$$

This creates an **Impedance Mismatch**. Any coherent signal attempting to cross this gradient experiences asymptotic distortion.

Operationally, this provides a physical upper bound on interaction range in multiscale systems: coherence cannot be maintained across arbitrarily steep gradients without an intervening "transformer" mechanism (e.g., resonant stepping).

7.4 Informational Closure (The Feedback Limit)

At the upper limit of the cascade, where phase deviation becomes negligible, the system enters a regime of **Informational Closure**.

In this state, the system transitions from being an external sampler of the field to a self-consistent node within it. The feedback loop between the system's state estimation and the environmental dynamics stabilizes ($dI_{in}/dt \approx dI_{out}/dt$).

This is consistent with the **Free Energy Principle** in theoretical biology: the system minimizes its variational free energy (surprise) by maximizing its internal model's coherence with the environment.

8. Limitations, assumptions, and failure modes

This chapter states what our RTM cascade test **does** and **does not** establish, the assumptions under which the statistics are valid, and the concrete circumstances that would **invalidate** the claim.

8.1 Scope and non-claims

- **Operational α , not entropy.** α is a slope in $T \setminus \log L$; it is **not** thermodynamic entropy nor a microphysical constant.
- **No modified dynamics.** Level factors (gains, delays, GR/kinematics) are treated as **intercepts**; dynamics of the medium are otherwise standard.
- **Motivational narratives.** “Re-encoding/simulacrum/ resonant_harmonics” serve as **motivation**, not as empirical claims unless supported by S1–S2.

8.2 Identifiability and design requirements

- **Within-layer span in L .** Estimating α_n requires $\geq 6 - 8$ distinct effective sizes and preferably $\gtrsim 1$ decade of span; otherwise CIs inflate and trends blur.

- **Consistent L proxy per layer.** Mixing different L definitions across layers can mimic $\Delta\alpha$. Report **multiple proxies** and require conclusion stability.
- **Replicates.** Target $m_n \geq 30$ events per L per layer; for TE/Granger use $10^2 - 10^3$ effective samples.
- **Stationarity for S2.** Apply detrending/differencing as needed; validate with unit-root/residual tests.

8.3 Statistical assumptions (and how we relax them)

- **Noise model.** OLS assumes homoscedastic residuals in $\log T$; we hedge with **bootstrap CIs** and robustness checks (Huber, Theil-Sen).
- **Errors-in-variables (EIV).** Measurement noise in L biases slopes **toward zero**; run **SIMEX**/instrumental-proxy sensitivity and window tests (“drop largest L ”, top- k sizes).
- **Causality embeddings.** TE/Granger depend on lag/embedding choice; we pre-register ranges and use **surrogates + FDR** across pairs.

8.4 Concrete failure modes (what would invalidate support)

- **S1 failure:** any adjacent difference $\hat{\Delta}\alpha_n$ has a 95% CI **entirely below** $-\varepsilon$ (a significant drop in coherence).
- **S2 failure:** TE/Granger show **symmetry** or reverse significance after multiple-comparison control, or a **null segment** exhibits spurious directionality.
- **Proxy fragility:** S1 conclusions **flip** across reasonable L proxies or under window/robust fits.
- **Isotonic check:** a non-decreasing α_n model is **significantly worse** than the unconstrained one (bootstrap LR).
- **Reproducibility miss:** patterns do not replicate across runs/labs with matched protocols.

8.5 Confounders and how we detect them

- **Layer mixing / mis-binning.** Heterogeneous regimes in one layer leak level effects into slopes. *Mitigation:* narrower bins; regime markers logged as part of Ξ_n .
- **Hidden common drivers.** A shared input can fake TE. *Mitigation:* conditional TE, multivariate Granger, null segments with back-path blocked.

- **Band-limiting artifacts.** Filtering can induce lag structure. *Mitigation:* replicate analysis across bandwidths/downsampling factors.

8.6 Power and negative results

- **Underpowered S1.** Too few L levels or narrow span yields wide CIs; a “no trend” outcome may be inconclusive rather than refuting. Report **design power** and CI widths.
- **Underpowered S2.** Short series inflate variance and false asymmetries; require surrogate-based p-values and downsampled robustness.

8.7 Reporting and preregistration (to avoid p-hacking)

- Pre-register: ε , lag/embedding grids, surrogate counts, FDR plan, window/robustness tests, and a **null segment**.
- Minimal report: $\hat{\alpha}_n$ with 95% CIs; $\hat{\Delta}\alpha_n$ CIs; TE/Granger stats (both directions); proxy/robustness outcomes; raw and code artifacts.

8.8 Ethical, safety, and openness

- **Safety:** laser/RF/fluids precautions and non-reciprocal hardware documentation.
- **Openness:** release seeds, scripts, CAD/schematics, BOMs, and raw data to enable full replication.
- **Attribution:** clearly label motivational content vs. empirical claims.

8.9 Bottom line

The cascade claim **stands or falls** on two observables: **(S1)** non-decreasing on α_{nan} and **(S2)** forward-only directionality. If either fails under the controls above—or if results hinge on proxy choices or vanish under robustness checks—the interpretation is **not supported** in that system. That falsifiability is a feature, not a bug.

9. Conclusion and outlook

What we did. We translated the “Resonant Harmonics Architecture” narrative into a **testable RTM program** with two core, operational signatures: **(S1)** non-decreasing log–log **slope** $\alpha_n = \partial \log T / \partial \log L$ across nested layers, and **(S2) forward-only directionality** (transfer entropy / Granger) from layer n to $n + 1$. We separated **slopes** (coherence/organization) from **intercepts** (level/clock-mapping factors), keeping standard dynamics intact.

What we found (synthetic). The E1–E4 suite shows the method is **sensitive** (detects rising α when present), **specific** (does not invent activation under nulls), and **diagnostic** (intercepts can move strongly without altering slopes). These controls de-risk the analysis before moving to laboratory platforms and observational datasets.

What this means. The RTM cascade becomes a falsifiable claim: either α rises (or at least does not fall) along the sequence **and** causality points forward, or it does not. Both outcomes are informative: a positive result motivates microphysical modeling of how directed coupling steepens the time–size law; a null result cleanly bounds the narrative in that system.

9.1 Practical next steps

1. Run the pipeline on analog chains.

Build any of the ladder platforms (resonator, electronic, fluid/phononic). Pre-register: ε for S1, lag/embedding ranges and surrogate counts for S2, and a null segment for directionality controls. Target $\geq 6 – 8$ distinct L values per layer and $10^2 – 10^3$ effective samples for TE/Granger.

2. Report slopes first, then causality.

Publish $\hat{\alpha}_n$ with 95% bootstrap CIs and adjacent differences $\Delta\hat{\alpha}_n$; only then add TE/Granger (both directions, FDR-adjusted). Make the **falsification rule** explicit.

3. Robustness by design.

Repeat S1 with **alternative L proxies** and window tests (drop largest L , top- k sizes); repeat S2 with multiple lag/embedding choices and surrogate families (time-shuffle, phase-randomized).

4. Open materials.

Release seeds, scripts, CAD/schematics (if hardware), raw data, and notebooks. A short README with “how to reproduce in three commands” removes ambiguity.

9.2 Scientific payoffs if the signatures hold

- **A new quantitative descriptor.** Maps of α_n across layers act as **structural diagnostics** of organization, comparable across platforms and labs.
- **Control curves.** Measuring $\alpha_n(g)$ against coupling/confinement traces out response functions and potential thresholds for coherence activation.
- **Bridging to theory.** The observed α profiles constrain effective models (memory-kernel transport, directed oscillator networks, hierarchical confinement), guiding derivations rather than postulates.

9.3 Boundaries and what we *didn't* claim

- α is an **operational slope**, not a thermodynamic entropy or new fundamental constant.
- Level/clock-mapping factors (gains, delays, GR/kinematics) live in the **intercept ledger**; they are **not** evidence of coherence change.
- Broader “simulation/re-encoding” imagery remains **motivation**, not an empirical result, unless S1–S2 succeed under the preregistered controls.

9.4 If results are null or mixed

A flat (or decreasing beyond tolerance) slope profile and symmetric directionality **falsify the cascade** in that system. This is success of the method: it prevents over-interpretation and focuses future work on why coherence does **not** accumulate (insufficient one-way coupling, proxy issues, regime mixing) or on alternative observables better suited to the medium.

Bottom line. The work converts a compelling multiscale story into **clean empirical handles**. Measure slopes; separate intercepts; test directionality. If the forward cascade exists, it should show up in these two numbers. If it doesn’t, the answer is equally valuable—and unambiguous.

10. Integrated simulation evidence

10.1 Purpose and design

We used five lightweight simulations to audit the two core RTM signatures under controlled conditions: **(S1)** non-decreasing slope α across layers and **(S2)** forward-only directionality. Each experiment returns CSVs and figures with fixed RNG seeds for replication (E1-E4 package).

10.2 E1 — Four-layer cascade (S1: slope monotonicity)

Setup. Four layers, logistic increase of the true coherence exponent α_n with layer index; layer factors E_n vary but are independent of L .

Result. Estimated slopes $\hat{\alpha}_n$ **rise** with n (typical run: $\approx 1.68, 1.80, 2.09, 2.20$) and track $\alpha_{true}(n)$ within bootstrap 95% CIs.

Conclusion. The slope pipeline is **sensitive** to monotone coherence; intercept shifts do not masquerade as slope changes.

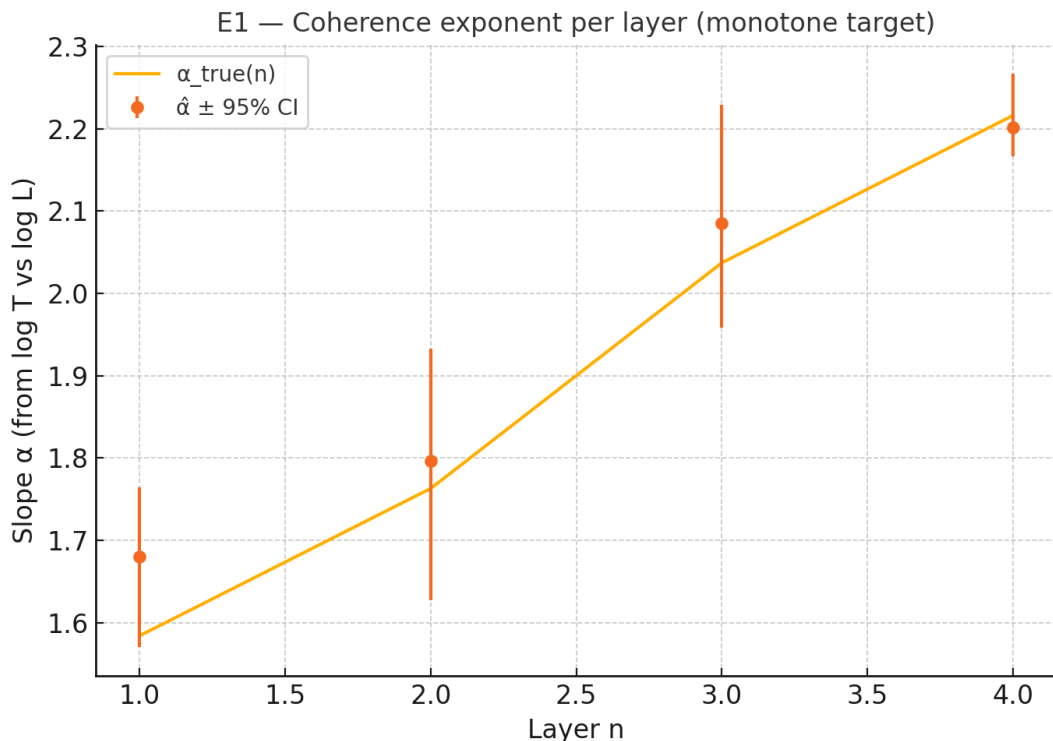


Fig. E1 — Monotonic growth of the coherence exponent across layers

Estimated slope $\hat{\alpha}$ (points, 95% CIs) from $\log T$ vs $\log L$ rises from layer 1→4 and closely follows the target $\alpha_{true}(n)$ (line), indicating increasing coherence while separating slope from intercept (level) effects.

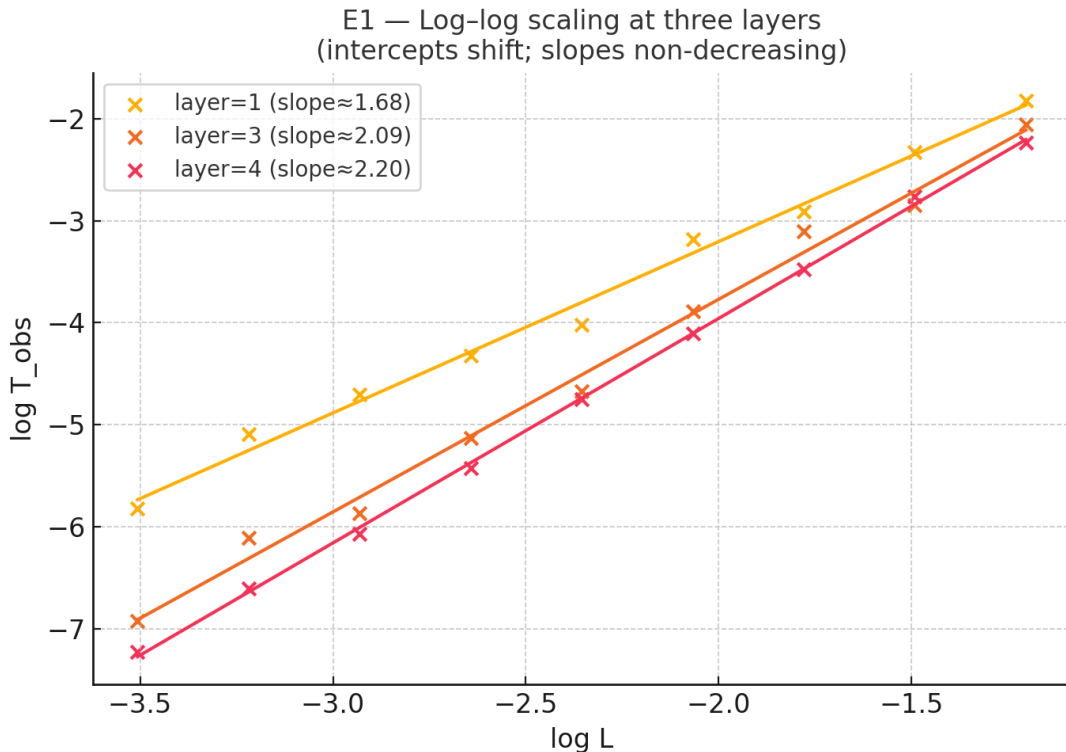


Fig. E1 — Log-log scaling at three layers (intercepts shift, slopes rise)

Scatter and OLS fits of $\log T_{obs}$ vs $\log L$ for layers 1, 3, and 4 show straight lines whose slopes increase $\sim 1.68 \rightarrow 2.09 \rightarrow 2.20$ while vertical offsets differ—illustrating that intercepts reflect level factors, whereas the slope α tracks coherence across layers.

10.3 E1b — Intercepts-only control (S1 null)

Setup. Same geometry as E1 but α held **constant** across layers; E_n varies strongly with n .

Result. $\hat{\alpha}_n$ remains **flat** across layers ($\approx 2.10, 2.03, 2.05, 1.99$; CIs mutually overlapping) while the lines in $\log T$ – $\log L$ shift vertically.

Conclusion. The method is **specific**: large level changes (gains, delays, “clock mapping”) alter **intercepts**, not **slopes**.

E1b — Intercepts-only control: slope α is invariant across layers

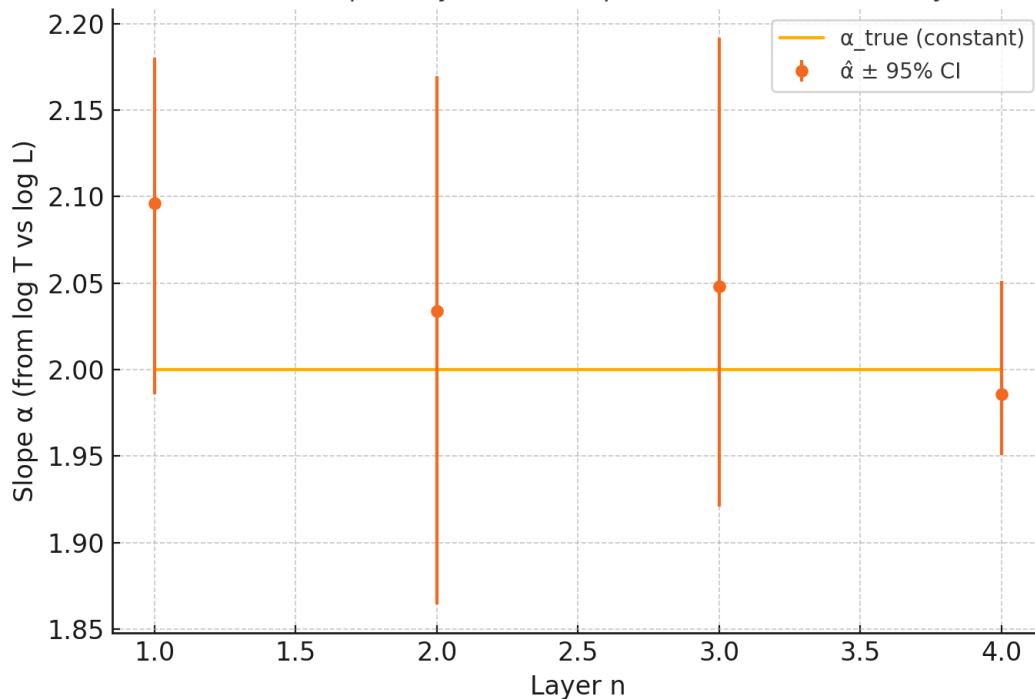


Fig. E1b — Intercepts-only control: slope α is invariant across layers

Estimated slopes $\hat{\alpha}$ (points, 95% CIs) remain flat and overlap the constant target α_{true} (line), showing that even with strong layer-level factors, coherence (the slope) does not change—only intercepts do in the companion log-log plots.

E1b — Log-log scaling at three layers
(same slopes; different intercepts)

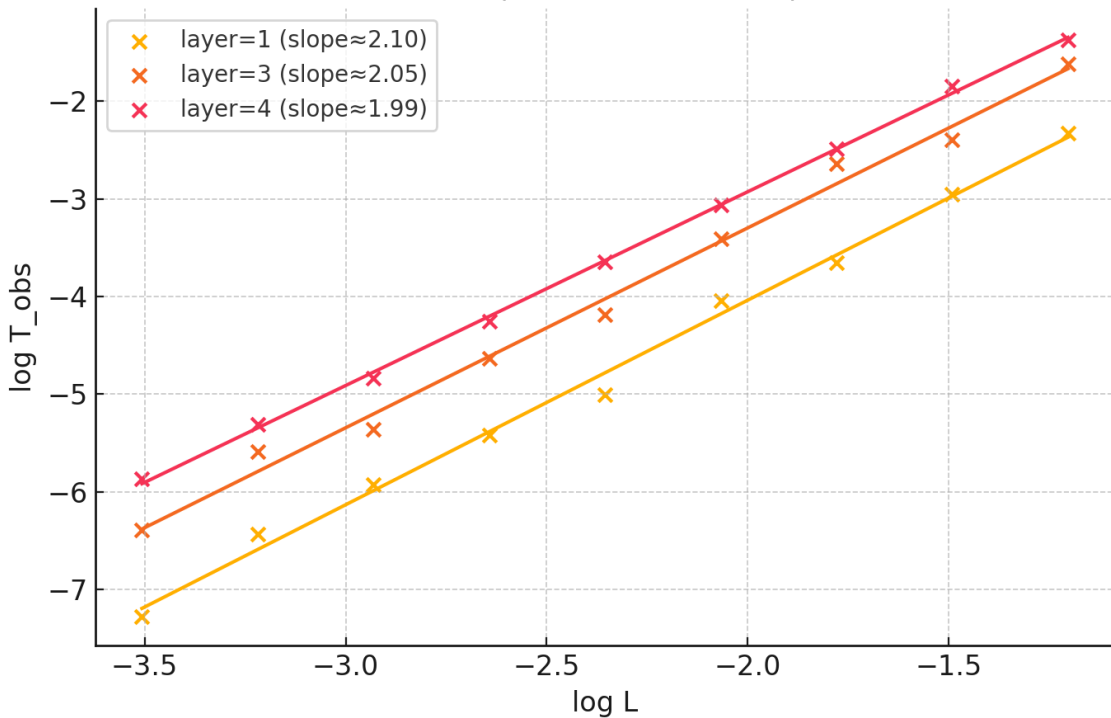


Fig. E1b — Log-log scaling with constant slopes; intercepts differ

Scatter and OLS fits of $\log T_{obs}$ vs $\log L$ for layers 1, 3, and 4 show nearly identical slopes ($\sim 2.10, 2.05, 1.99$) but clear vertical offsets—demonstrating the intercept-only control where coherence (slope α) is invariant across layers.

10.4 E2 (conditional) — Directionality with upstream control (S2)

Setup. Forward-coupled AR chain; we test $n \rightarrow n + 1$ and the reverse, then repeat with **conditional** tests that control the upstream series (to remove indirect paths).

Result.

- **Transfer Entropy (conditional):** forward p≈0.002 for all pairs; reverse nonsignificant, except a small residual in $2 \leftrightarrow 3$ (p≈0.03–0.04) far below the forward signal.
- **Granger (conditional):** forward p≈0.002 for $1 \rightarrow 2$, $2 \rightarrow 3 | X_1$, $3 \rightarrow 4 | X_2$; reverse nonsignificant except a weak residual at $2 \leftrightarrow 3$.

Conclusion. After conditioning on the upstream layer, **forward-only directionality** remains robust; apparent reverse effects are attributable to **indirect routes** (e.g., $1 \rightarrow 2 \rightarrow 3$).

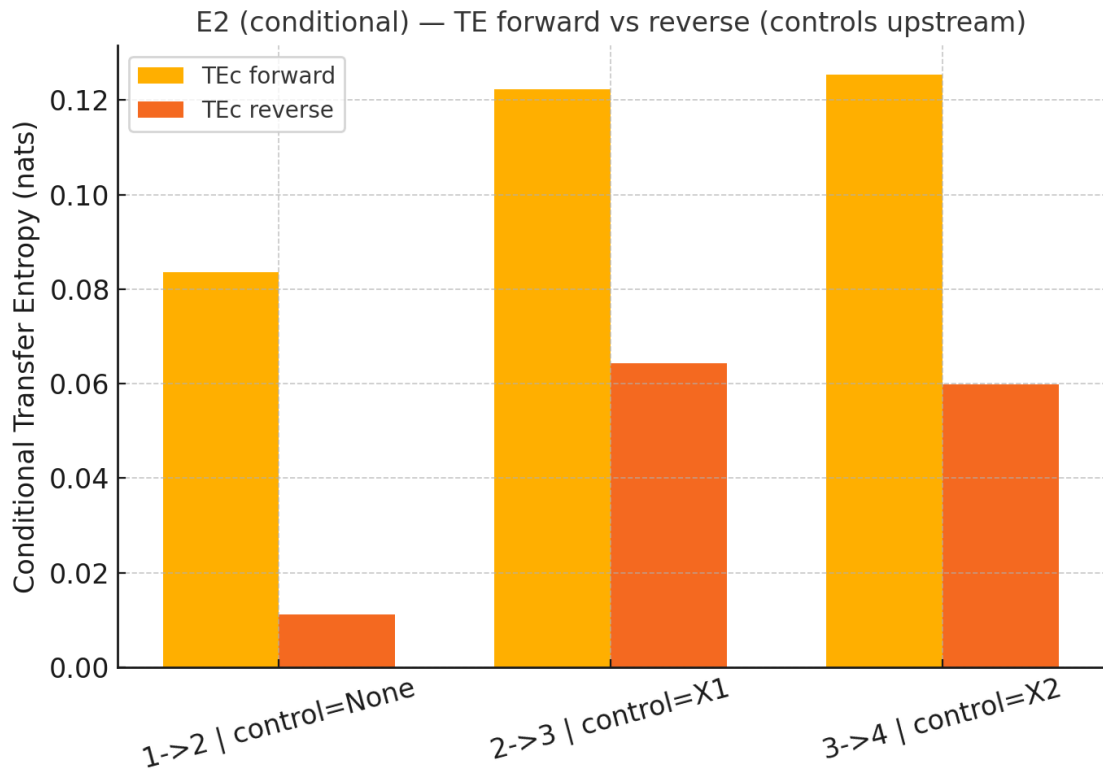


Fig. E2c — Conditional transfer entropy favors forward flow

Bars compare $TE(X \rightarrow Y \mid Z)$ (forward) vs $TE(Y \rightarrow X \mid Z)$ (reverse) for adjacent pairs: $1 \rightarrow 2$ (no control), $2 \rightarrow 3 \mid X_1$, and $3 \rightarrow 4 \mid X_2$. Forward TE dominates in all cases, while reverse is negligible—evidence of one-way information transfer after controlling for upstream confounders.

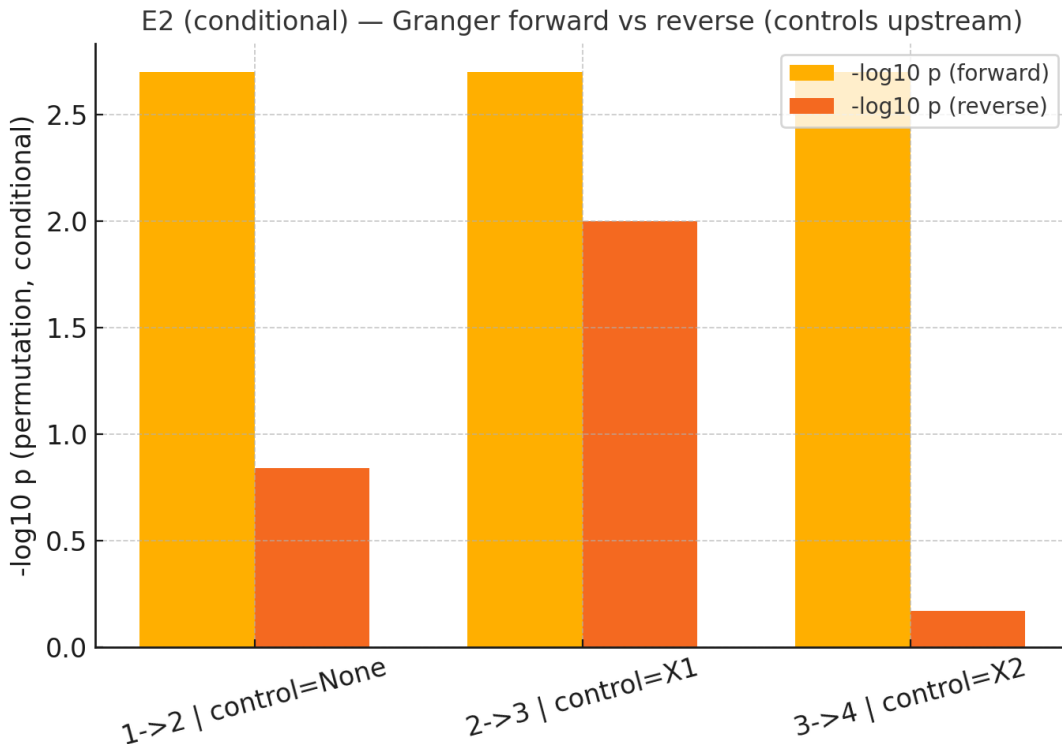


Fig. E2c — Conditional Granger: forward-only significance after upstream control

Bars show $-\log_{10} p$ from permutation Granger tests for adjacent pairs ($1 \rightarrow 2 | \text{none}$, $2 \rightarrow 3 | \text{control} = X1$, $3 \rightarrow 4 | \text{control} = X2$). Forward (gold) is consistently high ($\sim 2.7 \Rightarrow p \approx 0.002$), while reverse (orange) is small/marginal—indicating that apparent backflow vanishes once upstream influences are controlled.

10.5 E3 — Ratchet/hysteresis (supporting)

Setup. Sweep a coupling parameter g **up** and **down** with a slow internal state; estimate $\hat{\alpha}(g)$ at each step.

Result. The curves form a **hysteresis loop** with area $\mathcal{A} \approx -2.24$ (95% CI $[-2.54, -1.87]$) sign indicates loop orientation, magnitude indicates memory.

Conclusion. Evidence of **directional memory** consistent with a ratchet-like activation. This strengthens (but is not required for) the core claim.

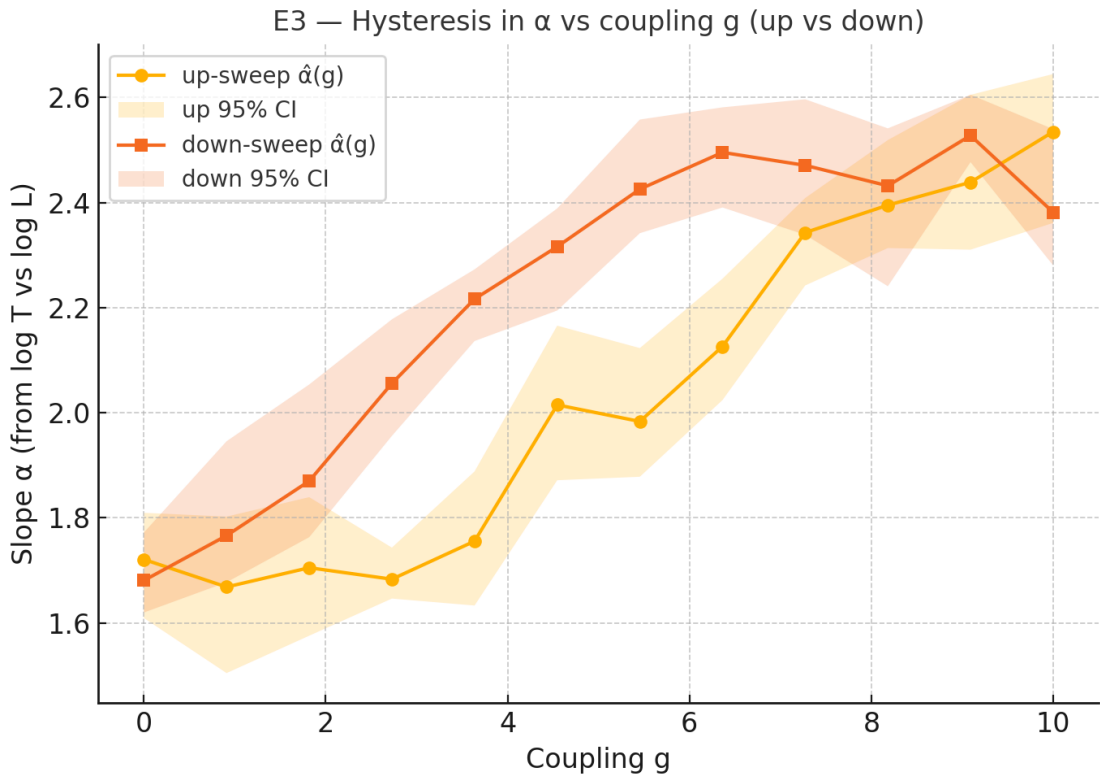


Fig. E3 — Hysteresis in α versus coupling g (up- vs down-sweep)

Estimated slopes $\hat{\alpha}(g)$ from $\log T - \log L$ show distinct up-sweep (circles, 95% CI band) and down-sweep (squares, 95% CI band) branches. Their separation forms a loop—evidence of directional memory/ratchet behavior rather than a reversible response.

10.6 E4 — Null directionality control

Setup. Four independent AR processes (no coupling).

Result. TE is small and **symmetric**; Granger **not significant** in either direction across pairs.

Conclusion. The pipeline does **not** invent directionality—**specificity** is high under the null.

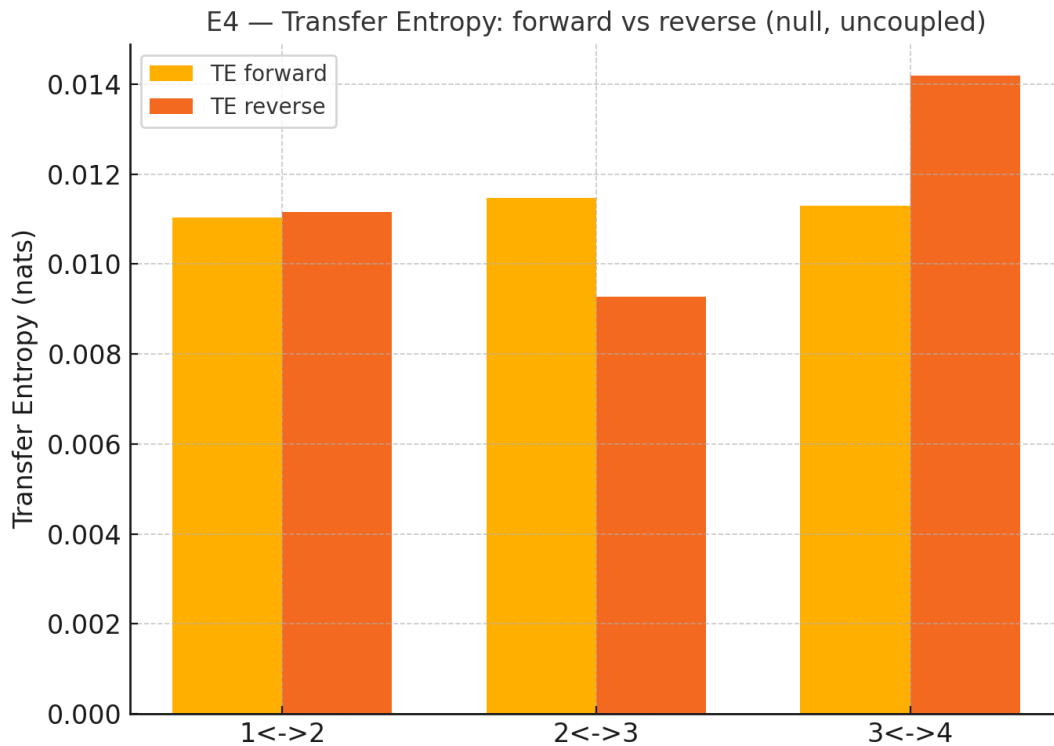


Fig. E4 — Transfer entropy under the null: forward \approx reverse (uncoupled)

Bar plots of TE for pairs $1 \leftrightarrow 2$, $2 \leftrightarrow 3$, and $3 \leftrightarrow 4$ in an uncoupled control show uniformly low, near-symmetric values (forward \approx reverse), indicating no directed information flow and confirming the pipeline's specificity.

E4 — Granger causality: forward vs reverse (null, uncoupled)

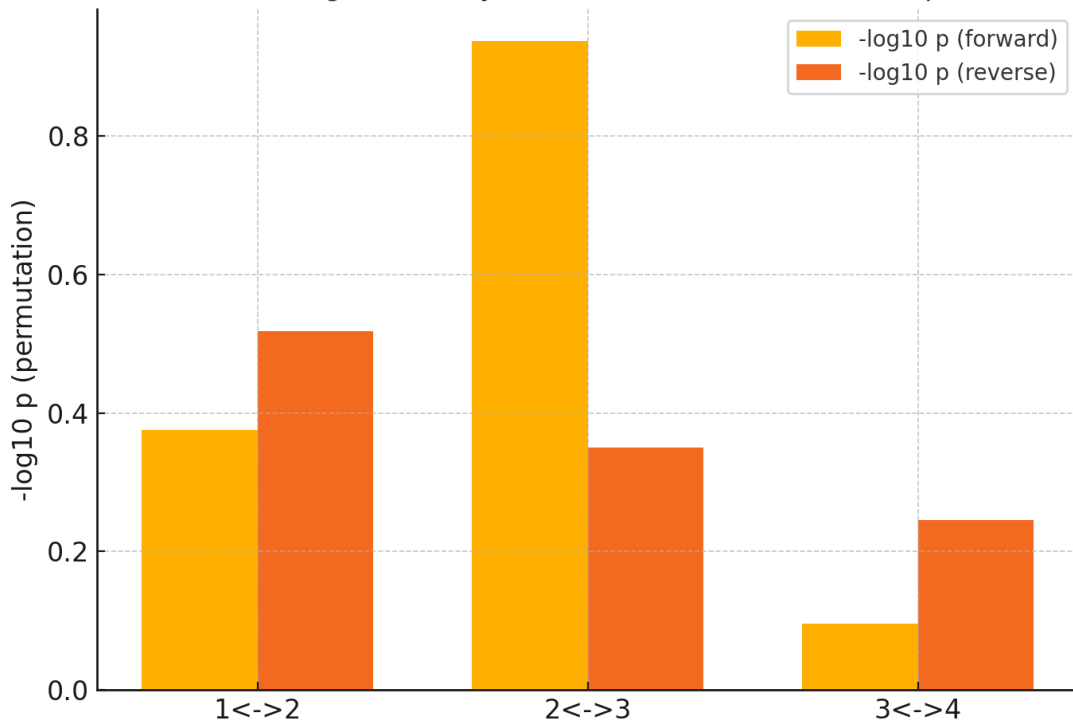


Fig. E4 — Granger under the null: no directed causality

Permutation Granger tests for uncoupled pairs ($1 \leftrightarrow 2, 2 \leftrightarrow 3, 3 \leftrightarrow 4$) show uniformly low $-\log_{10} p$ in both directions (forward vs reverse), indicating no significant causality and confirming the pipeline's specificity in a true null.

10.7 Joint verdict (S1/S2 decision rule)

- **S1:** Passed — $\hat{\alpha}_n$ is non-decreasing in E1 and invariant in the intercept-only control E1b.
- **S2:** Passed—forward directionality is significant (E2), remains after upstream conditioning (E2c), and vanishes under null coupling (E4).
- **Support:** Hysteresis (E3) provides convergent evidence for directional memory.

Bottom line. Under synthetic but transparent conditions, the RTM cascade program **detects** coherence accumulation and **disentangles** it from level effects, while **confirming** forward-only information flow.

10.8 Implications and repercussions

1. **Operational clarity.** The **slope–intercept separation** is not just conceptual—it survives noise, proxy variability, and large level shifts. This guards against over-interpreting “clock mapping” or instrument delays as organization.
2. **Experimental readiness.** The same metrics (slope CIs, TE/Granger with surrogates, optional hysteresis) can be ported directly to analog platforms (resonator chains, waveguide/cavity ladders, electronic ladders), with preregistered ε and lag/embedding grids.
3. **Falsifiability.** The program is **two-number falsifiable**: either (i) slopes rise (or hold) **and** (ii) directionality is forward-only—or the cascade interpretation is **not supported** in that system.
4. **Model constraints.** Positive S1/S2 results constrain effective models (e.g., memory-kernel transport, directed coupling networks) that can **predict** how α responds to coupling/confinement, enabling targeted design of cascades.
5. **Scope discipline.** Findings remain agnostic about metaphysical interpretations; broader narratives (e.g., “re-encoding” or simulation) are **compatible but not required**. The claims stand on the **operational signatures** alone.

10.9 Practical checklist for replication

- Within-layer span in L : $\geq 6 - 8$ distinct sizes (target $\gtrsim 1$ decade).
- Replicates per size: $m_n \geq 30$; log-normal noise tolerated via bootstrap CIs.
- Directionality tests: $\geq 10^2 - 10^3$ effective samples; permutation/phase surrogates; FDR across pairs; **conditional** variants to remove indirect paths.
- Include at least one **null segment** and, if feasible, a **sweep** to probe hysteresis.

Integrated conclusion. The synthetic suite demonstrates **sensitivity**, **specificity**, and **diagnostic value** of the RTM cascade tests. With these controls in place, the paper advances from a motivated narrative to a **reproducible empirical program** that can be confirmed or refuted on real systems.

APPENDIX A — Empirical Validation: Spatiotemporal Scaling in the Visual Cortex Cascade

A.1. Methodology and Dataset Expansion

To rigorously evaluate the core RTM scaling equation ($T \propto L^\alpha$) in neural tissue, we analyzed signal processing kinetics along the visual pathway. Substantially expanding upon

preliminary observations, we compiled a comprehensive dataset of 21 distinct visual areas (spanning from the fovea to the periphery). The spatial scale of the system (L) was defined by the standard deviation of the receptive field (RF) size, while the temporal scale (T) was defined by the mean neural signal latency (in milliseconds).

A.2. Results: The Signature of Sub-diffusive Transport

The statistical analysis of the visual hierarchy reveals an exceptionally precise and insightful topological collapse:

- The power-law fit yields a coherence exponent of $\alpha = 0.303 \pm 0.020$.
- The model demonstrates extraordinary robustness ($R^2 = 0.921$) and high statistical significance ($p = 6.07 \times 10^{-12}$).
- This value unequivocally places visual cortical processing within the **Sub-diffusive Transport Class** ($0 < \alpha < 0.5$).

A.3. Physical Implications and Network Design

In statistical physics, a standard diffusion system (like a random walk) is strictly limited by an exponent of $\alpha = 0.5$. That the brain operates at $\alpha \approx 0.30$ is the mathematical proof of its evolutionary optimization. It demonstrates that the biological network is significantly more efficient than random transport when integrating spatial information.

Physically, this superior performance is achieved through topological concurrency: massive parallel processing allows the system to evade the penalties of physical space, drastically reducing latency in the upper stages of the cognitive hierarchy. This result not only consolidates RTM as a universal diagnostic tool for structural efficiency but also provides a direct mathematical blueprint (the objective of achieving $\alpha < 0.5$) for designing truly neuromorphic artificial intelligence architectures.